Theor Chem Acc (2007) 118:253–264
DOI 10.1007/s00214-007-0318-2

REGULAR ARTICLE

Germyl mesolytic dissociations in the allylgermane and penta-2,4-dienylgermane radical anions. A theoretical study

Paola Antoniotti · Claudio Carra · Andrea Maranzana · Glauco Tonachini

Received: 17 November 2006 / Accepted: 6 March 2007 / Published online: 6 June 2007

Abstract In CH_2CHCH_2–$GeH_3^{\cdot -}$ two stable structures have a trigonal bipyramidal arrangement around Ge, with the extra electron in equatorial (tbp eq) or axial (tbp ax) position. In $CH_2(CH)_3CH_2$–$GeH_3^{\cdot -}$ only tbp ax is found, while a second structure with a tetrahedral germyl group has the extra electron on the conjugated π system. C−Ge bond cleavage yields allyl/ pentadienyl radicals plus germide. Both dissociation reactions require 4–6 kcal mol^{-1}, less than the analogous C and Si systems (ca. 30 and 14 kcal mol^{-1}, respectively). Fragmentation is dramatically activated with respect to homolysis in the corresponding neutrals. The wavefunction is dominated by one single configuration at all distances, in contrast to homolytic cleavage, in which two configurations are important. C−Ge bond dissociation is at variance also with heterolysis, due to spin recoupling of one of the C−Ge bond electrons with the originally unpaired electron.

Keywords Mesolysis · Radical anions · Allylgermane · Pentadienylgermane · Activation

Contribution to the Fernando Bernardi Memorial Issue.

P. Antoniotti · A. Maranzana · G. Tonachini (✉)
Dipartimento di Chimica Generale e Organica Applicata,
Università di Torino, Corso Massimo D'Azeglio 48,
10125 Torino, Italy
e-mail: glauco.tonachini@unito.it

C. Carra
Universities Space Research Association,
NASA-JSC Space Radiation Health Project, 2101 NASA Parkway,
Houston, TX 77058, USA

Present Address:
A. Maranzana
Department of Atmospheric, Oceanic, and Space Sciences,
University of Michigan, Ann Arbor, MI 48109-2143, USA

1 Introduction

Radical ions can be obtained from neutral precursor molecules by different methods, including photoionization and photoinduced electron transfer (PET) [1–3], electrochemical [4–7] or pulse radiolytic [8,9] methods, and chemical ionization [10,11]. A vast literature has accumulated on the chemical dynamics and reactivity of these odd-electron species [12–14], which has also led to synthetically useful chemical reactions [15–18][1]. In particular, use can be made of fragmentation [1–3], for instance as a mechanistic probe to detect electron transfer in biological or organic reactions [19–21]. The radical anions, called *hypernomers* because they have one electron more than some precursor molecules [22], can often undergo fragmentation into a radical and a charged species, as do the analogous radical cations (similarly called *hyponomers*). In this respect, they exhibit some enhancement of reactivity (*activation*) with respect to their neutral parent molecules [22–25]. Within a localized picture, it could be supposed that the breaking σ bond is weakened, and activated toward cleavage, by one extra electron associated to it. However, the molecular systems studied experimentally [23–35] are commonly made up by an arylic or allylic π subsystem, β to the σ bond involved in the fragmentation. This π subsystem is connected through the σ bond to another part of the molecule, Y, which can also be (in part) an unsaturated subsystem. Two examples of radical anion fragmentation involving different systems [23–26] are shown in Scheme 1 (cleaved bond marked by an arrow).

[1] The reductive cleavage of Sn–Sn bonds is a procedure used to generate R_3 Sn- (see [18]). Radical anions can be intermediates of these fragmentations.

Scheme 1 Examples of radical anion fragmentations

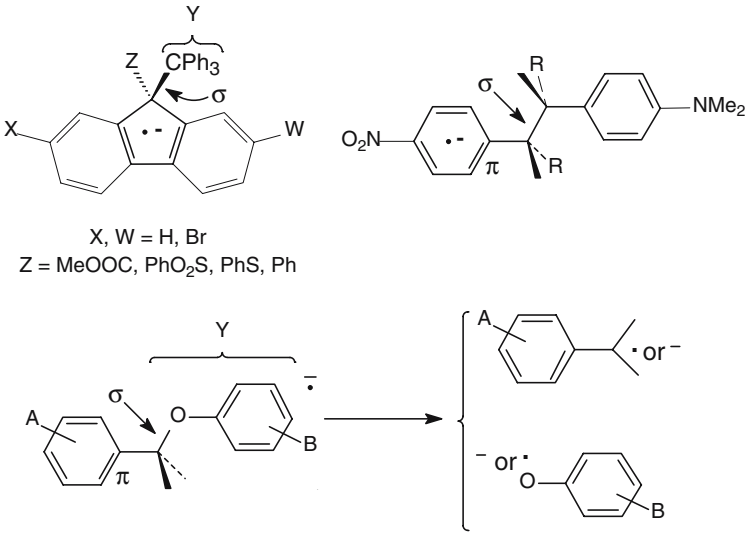

In other cases, as in dihaloalkanes, electron transfer and bond cleavage are concerted, ruling out the intermediacy of radical anions [23–35].

Interesting and synthetically useful chemistry has been developed from the cleavage of radical cations from group IVA organometallics (–C–MR_3; M = Pb, Sn, Si, Ge) [10,11] and also mesolysis of Me_3Sn–MMe_3 (M = Sn, Ge, Si) [15–18]. However, no report is available on the generation and fragmentation of radical anions from M–M bonds.

Some possible ambiguity about the *formal* partitioning in the anion radical of either two or three electrons pertaining to this dissociating bond exists, and seems to justify the introduction of the word *mesolysis* for this process [23–25]. It is of theoretical interest to define the nature of the weakened σ bond cleavage process, and to compare its features to those of a typical homolytic or heterolytic fragmentation.

Some theoretical studies by other groups, dealing with the cleavage of organic radical anions, have appeared up to now [36–45]. In two theoretical studies carried out in this laboratory, the nature of the σ_{CC} or σ_{CSi} bond cleavage process was examined, in cyclic [46] or open-chain [47] radical cations and anions. The features of these fragmentations were compared on the basis of the wavefunction and electron distribution changes. The purpose of the present study is to extend the investigation to the σ_{CGe} bond cleavage process, in open-chain C_1 unsaturated organic radical anions substituted by a germyl group. The two systems examined in this paper are displayed in Chart 1. Both possess two potential electron acceptor sites: one is the unsaturated part of the organic molecule, the other the C–GeH_3 group (which can possibly undergo a geometrical change, from tetrahedral to trigonal bipyramidal).

Therefore, in the present study, the possibility of accepting the extra electron in two different rather localized fashions is inspected (point 1). If extending the unsaturated part is

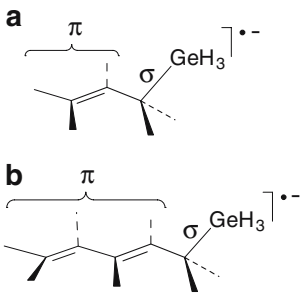

Chart 1 The two radical anion systems under study

expected to enhance its ability to compete with the C–GeH_3 part in accepting the extra electron, its localization on the π subsystem, on the other hand, should not *directly* weaken the bond to be broken. By contrast, its localization onto the germyl group is expected to act so *directly*, and promote dissociation, because it contributes to populate an orbital endowed with C–GeH_3 antibonding character, as will be discussed in the "Results". Therefore, the reasons of the *activation* observed in the hypernomers with respect to their neutral precursors (point 2), as well as the nature of the cleavage (point 3) will be discussed. Finally, the **a** and **b** germyl-containing radical anions will be compared with the similar and previously studied methyl and silyl systems [47], as regards the energetic features of the cleavage reaction, the nature of the wavefunction, and the traits of the electron distribution along the reaction pathway (point 4).

2 Methods

The study of the fragmentation reactions of the **a** and **b** radical ions shown in Chart 1 was performed by defining the stable and transition structures (TS) corresponding to

critical points on the relevant energy hypersurfaces. These structures were optimized without constraints using gradient optimization procedures [48–51] at the complete active space multi-configuration self consistent field (CAS-MCSCF) [52–54] level of theory, with the polarized split-valence shell 6-31G(d) basis set [55–59]. In correspondence to the CAS-MCSCF critical points, NAO group charges [60–65] were computed to discuss the electron distribution.

In these calculations the active space chosen consists of those orbitals which can be thought of as more directly involved in bond cleavage process. Within the active space a complete CI is carried out, and in correspondence to its wavefunction the molecular orbitals are optimized. Two active spaces were used for the allylgermane radical anion. The first one has nine electron in eight orbitals and is labeled as (9,8). A corresponding (8,8) active space was used for the relevant neutral system. For the separated products, allyl and germyl, the eight orbitals consisting of the three-term π system of the CH_2CHCH_2 moiety were chosen, together with the four germyl orbitals of σ_{GeH} or σ^*_{GeH} nature (usually labeled for a C_{3v} "object" as π_{GeH_3}, $\pi^*_{GeH_3}$ and π'_{GeH_3}, $\pi'^*_{GeH_3}$ because of their nodal properties), and finally either the s–p hybrid of the GeH_3^- anion, pointing away from the hydrogens, $\sigma^{out}_{GeH_3}$ or a pure p_{Ge} orbital in the $GeH_3^\bullet$ radical, if the less stable dissociation limit is considered. For the reagent, the eight orbitals consist of the π_{CC} and π_{CC^*} system pertaining to the double CC bond, the σ_{CGe} and σ^*_{CGe} system of the bond to be cleaved (these π and σ orbitals are in fact mixed to some extent in the reactants), and to the just mentioned GeH_3 π, π^* and π', π'^* couples, two of which filled. The extra electron is found in the σ^*_{CGe} orbital, which has a significant contribution from a further Ge-centered lobe (axial or equatorial, depending on the geometry). To explore the dependence of the geometrical parameters from the active space, a smaller (5,4) active space, in which the π, π^* and π', π'^* couples were discarded, was also used to recompute the geometries of the more stable minimum, the TS, and the dissociation limit. Thus the (5,4) space is just made, for the reagent, by the π, π^* couple of the double CC bond, plus the σ, σ^* couple of the bond that cleaves. The extra electron is again found associated to the σ^*_{CGe} orbital, which maintains the features it has within the (9,8) space. For the resulting fragments, this translates to the three-term π system of allyl plus the $\sigma^{out}_{GeH_3}$ orbital of germyl.

When extending the π system of the unsaturated part from (2,2), as for the unique double bond in the allylgermane radical ion, to (4,4) for the conjugated π system in the pentadienylgermane radical anion, the active space was forcedly reduced in the germyl part of the system. The chosen active orbitals are, for the reagent, just the (4,4) π system of the conjugated carbon-carbon double bonds, together with the σ_{CGe}, σ^*_{CGe} system of the bond to be cleaved (again, the π and σ orbitals are mixed to some extent in the reactants). For the separated pentadienyl and GeH_3 products this choice corresponds to the five-orbital π system of the former fragment, and to a $\sigma^{out}_{GeH_3}$ hybrid (or a p_{Ge} orbital) for the latter. This choice defines for the radical anion an active space of seven electrons in six orbitals, labeled as (7,6), which corresponds to a (6,6) active space for the relevant neutral system. The (7,6) space for pentadienylgermane corresponds to the (5,4) space tested for the allylgermane system.

The CAS-MCSCF theory level is expected to take into account a large share of the structure-dependent (or non-dynamical) correlation effects. In this study, it is used mainly to provide a readable wavefunction which enables us to examine the characteristics of the bond cleavage process. However, dynamic correlation effects on the reaction energetics have to be taken into account by some other approach. To define the energy values in correspondence of the CAS-MCSCF geometries, we chose the multireference second-order perturbative CASPT2 method [66,67], and (taking also into account that one electron configuration was found to be dominant all along the dissociation pathways) the unrestricted coupled cluster method [68–77] (which has, as a single reference, the UHF wavefunction). With the latter method, more complete dissociation profiles were defined by performing series of single-point energy calculations at the unrestricted CCSD(T) theory level, using CAS-MCSCF geometries obtained by constrained optimizations, carried out in correspondence to fixed C−Ge distances. This was done with the 6-311+G(d) basis set for both systems, and with the 6-311+G(2d,p) basis set only for the allylgermane radical anion, to test the dependence of the energy differences from the basis set [55–59]. These coupled cluster calculations were performed within the default "frozen core" approximation. At the CASPT2 level, only the energy differences relevant to the critical points of the allylgermane radical anion have been assessed. Also the CAS(5,4)-PT2 energy calculations were performed within the frozen core approximation, with the 6-311+G(d) and 6-311+G (2d,p) basis sets. The (5,4) active space is the same as defined above. Therefore, when discussing the energy barriers in the next section, we will make reference to the maxima and minima in the CCSD(T) energy profiles and to the CASPT2 energy differences[2].

All geometry optimizations and the coupled cluster calculations were executed by using the GAUSSIAN03 systems of programs [78]. The CASPT2 computations were performed by the MOLCAS 4 program [79].

[2] It must be prudently kept in mind that performing single-point energy calculations is a rather rough probing of the higher level energy hypersurface. This remark is particularly reasonable in the case of the transition structures, which can be found shifted when passing from one theory level to another.

3 Results and discussion

In this section, the features of the CAS-MCSCF wave function, which are apt to support a qualitative description and interpretation of the cleavage processes, will be discussed. On the other hand, as regards the energetics, we will consider the CCSD(T) and CASPT2 dissociation profiles.

3.1 Methylgermane radical anion

This section has the purpose of illustrating the effect of the addition of one extra electron to a simple Ge-centered molecule that does not possess a π subsystem, thus providing a reference for comparing the effects of a similar electron gain for the systems of Chart 1. The neutral methylgermane has almost tetrahedral arrangements around C and Ge (HCGe and HGeC angles of $110° - 111°$). In contrast, two energy minima are detected for the CH_3GeH_3 radical anion, with a geometrical arrangement around the Ge atom which suggests a trigonal bipyramidal (tbp) hybridization. One of the positions around Ge is occupied by an orbital lobe carrying the unpaired electron: this lobe can be in an approximate axial arrangement (tbp ax, for short), or in an equatorial arrangement (tbp eq).

3.1.1 Study of different active spaces

To examine this example, three active spaces are chosen. (1) The first and largest active space chosen is defined with the aim of describing the bonds around the Ge atom (the σ_{CGe} and σ_{GeH} bonds) by a rather complete set of valence group orbitals. The CAS thus defined is (9,8) and is taken as a reference for the tests that follow. The singly occupied molecular orbital (SOMO) is a σ^*_{CGe} orbital with a significant contribution of the axial or equatorial Ge lobe just mentioned. (2) With the second choice, the σ, σ^* couple of *a* symmetry pertaining to the GeH_3 fragment is dropped from the active space, and the space reduces consequently to (7,6). This second active space reflects the choice subsequently adopted for the GeH_3 group within the allylgermane system (see Sect. 3.2), for which, on the other hand, a π_{CC} and π^*_{CC} couple is also introduced [the active space is thus labeled again (9,8)]. The extra electron is found again in a σ^*_{CGe} orbital. (3) The third active space is limited to the σ, σ^* couple of the C−Ge bond (of which the latter has σ^*_{CGe} character, but has also a contribution from a Ge lobe), and thus is just (3,2). This more modest choice, together with the result that will be presently discussed, is introduced to justify the active space adopted to describe the larger pentadienylgermane system, for which, if we consider the (4,4) contribution of the π system, the active space is an overall (7,6).

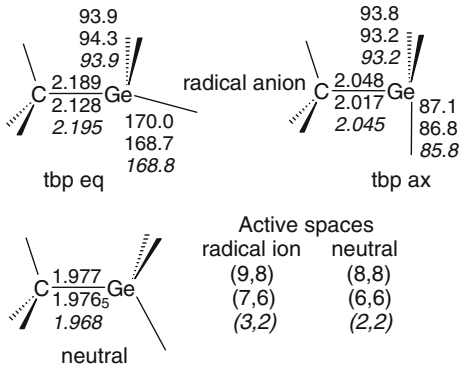

Chart 2 Some selected geometrical parameters for the stable structures of the methylgermane radical anion and corresponding neutral. Uppermost, median, and lowest figures are relevant to the active spaces indicated

The question is whether the more limited active spaces give geometries close to those defined by the reference (9,8) space.

The main geometrical features of the optimized radical anion minima are shown in Chart 2. The tbp eq minimum is lower in energy than the tbp ax by 5.8 kcal mol^{-1} [at CAS(9,8)], by 5.6 [at CAS(7,6)], and by 6.8 [at CAS(3,2)]. Notably, the extra electron placed in the σ^*_{CGe} orbital produces an elongation of the C−Ge bond with any active space. The more important geometrical parameters do not show large variations. This result offers a justification for treating the allylgermane not only, as said, with the more flexible (9,8) active space, but also with a more limited one, for sake of comparison. As regards the more extended radical ion, we had to limit ourselves to the smaller one (see "Methods").

3.1.2 Nature of the radical anion

Quantum chemical calculations describe methylgermane and the other two title radical anions by similar traits. These will be briefly discussed in the following for the former, to justify the computational level adopted in this study. All these radical anions are described as temporary anions, i.e. the corresponding neutrals exhibit negative electron affinities ($EA = E_{neutral} - E_{anion}$)[3]. Therefore, they can be expected to be electronically unstable, in the sense that, upon enlargement of the basis set by addition of increasingly more diffuse functions, they could suffer the so-called variational collapse. In other words, the extra electron would be found to populate the more diffuse functions, providing the picture of the neutral molecule plus a detaching electron. Figure 1 illustrates this point. Line 1 corresponds to a CAS energy profile for dissociation, obtained by using the 6-31G(d) basis set.

[3] For a discussion on species with negative vertical or adiabatic electron affinities, having the character of valence or not-valence anions, see [80].

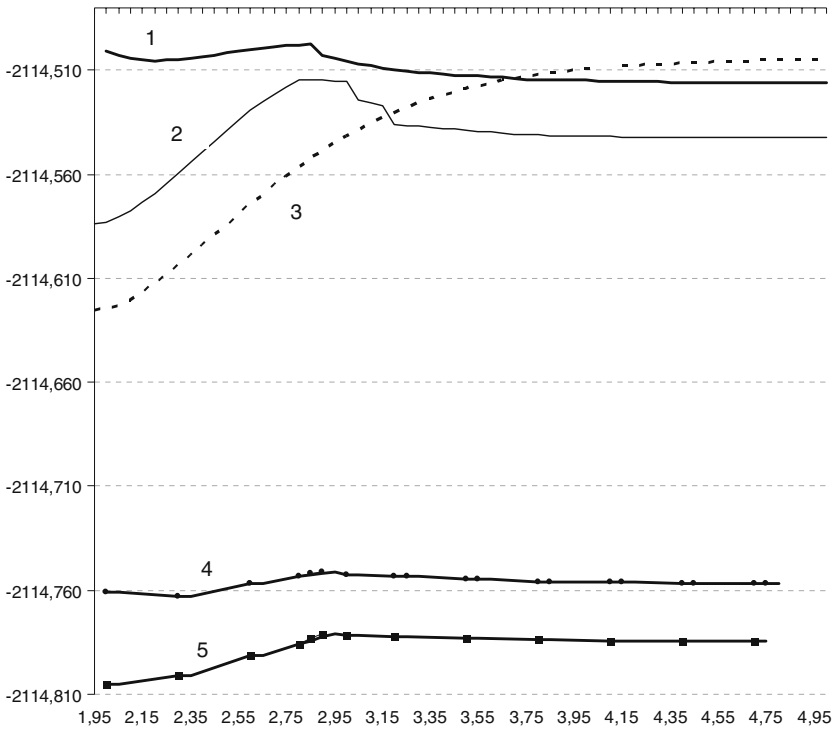

Fig. 1 *Upper lines* CAS(3,2)-MCSCF energy profiles (scans with optimization at each point; about 60 points reported) for the dissociation of the methylgermane radical anion, using the 6-31G(d) [1], or 6-31+G(d) [4–7] basis sets. The corresponding CAS(2,2) profile for the neutral is obtained with the 6-31+G(d) basis set [8,9]. *Lower lines* CCSD(T) energy profiles obtained with the 6-31G(d) [10,11] and 6-31+G(d) [12–14] basis sets. *Abscissa* C–Ge distance in Ångströms

The CH_3GeH_3 radical anion is described in this case as a valence anion, because the limited flexibility of the valence shell in 6-31G(d) does not allow it in a different way. Line 2 is a profile obtained with the standard 6-31+G(d) basis set, which contains diffuse sp functions. Line 3 represents the homolytic bond cleavage in the parent methylgermane. It is apparent that the leftmost part of the profile 2 parallels 3, while the rightmost part is close to 1. The behaviour of the system, as described by lines 1 and 2, is similar to what was obtained for the dissociation of $CH_3SH^{\cdot -}$ and $CH_3SCH_3^{\cdot -}$ by Dézarnaud-Dandine and Sevin [81], and could be discussed similarly. In brief, if diffuse functions are available, at short C−Ge distances the electron is loosely associated with what is basically the neutral molecule (it is not a valence radical anion). Then, at some point (the maximum zone, around 2.8 Å) it becomes associated with the dissociating system in a tighter way. At longer distances, it belongs to one of the two fragments (germide). If, on the other hand, no diffuse functions are available, the electron is artificially confined in a valence orbital at any C−Ge distance. Therefore, a question arises about the more correct basis set choice. We believe that it depends on the purpose of the theoretical study, and the artificial description forcing the valence anion nature could be the desired one, at least to obtain the geometries. In fact, if we intend, by these gas-phase calculations, to set up a model for situations in which the radical anion system is stabilized (e.g., from being in the condensed phase, by the interaction with a counterion), or to make reference to vertical electron attachment experiments [such as electron transmission spectroscopy (ETS)] [82], one should avoid describing electron ejection instead. This could be done computationally either by a "stabilization method", as the one proposed by Falcetta and Jordan [83], or by artificially limiting the extension of the basis set, as discussed by Guerra ("boxing procedure") [84–86]. One could consider, for instance, the comparison between computed and experimental EAs for $CH_3SH^{\cdot -}$ and $CH_3SCH_3^{\cdot -}$ in the mentioned paper by Dézarnaud-Dandine and Sevin [81]. Coming back to Fig. 1, it can be seen that the coupled cluster profiles, obtained by energy computation with basis sets with and without diffuse functions are rather similar. This can be attributed to the fact that both rely on geometries obtained *without* diffuse functions (e.g., the tbp eq structure). Apparently, imposing a geometry typical of a forced valence anion nature, is sufficient to compel that trait to the energy evaluation also.

3.2 Allylgermane radical anion

As for the methylgermane radical ion, two energy minima are detected on the potential energy surface of this system at the CAS(9,8)-MCSCF/6-31G(d) level of theory. Both radical anions show a trigonal bipyramidal (tbp) hybridation for the Ge atom. The tbp eq is the stablest structure. Its main geometrical parameters, and the NAO group charges pertaining to the two ideal portions of the radical anion (germyl and allyl), are shown in Fig. 2. The charge distribution is reflected by the variation of the more important geometrical parameter with respect to the neutral parent molecule. The

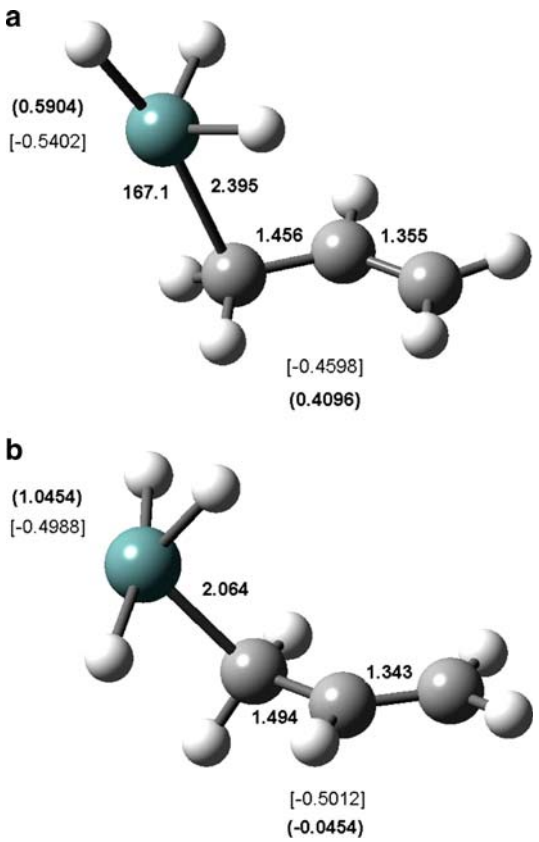

Fig. 2 Allylgermane radical anion: **a** tbp eq; **b** tbp ax. Main geometrical parameters, and NAO group charges (between brackets) for the germyl and allyl parts of the system. UHF group spin densities in parentheses

HGeC angles (167°, 92°, 94°) show that the system is nearly in an trigonal bipyramidal arrangement, with the extra electron localized in an equatorial position, and the C−Ge bond is elongated by 0.407 Å.

Again, the SOMO, which carries the extra electron, has a Ge-centered lobe in an approximately equatorial arrangement (tbp eq), as is displayed in Fig. 3a, or in an axial arrangement (tbp ax, Fig. 3b). This orbital is also σ-antibonding in character, in particular regarding the C−Ge bond to be cleaved, as seen in Sect. 3.1, but also regarding the π system (which recalls, however, more the π_2 orbital of an allyl system than the π^* of the double bond). Its shape and phases can be schematically rationalized in terms of the orbitals belonging to the idealized fragments GeH_3 and CH_2CHCH_2 (Chart 3). The SOMO is *approximately* corresponding to the out-of-phase combinations of the almost degenerate orbitals HOMO(GeH_3) and SOMO(allyl). In the case of tbp ax, by contrast, an antibonding nature of the SOMO cannot be observed.

The tbp eq structure is the most stable minimum (Table 1). The tbp ax minimum is higher in energy by 4.6 kcal mol^{-1} at the CCSD(T) level of theory (and 8.3 kcal mol^{-1} at the CASPT2 level of calculation). A conceivable third energy minimum, having the C–GeH_3 part of the molecule approximately tetrahedral, and the extra electron located on the vinyl part of the system, could not be found.

The two dissociation limits, corresponding to different apportionments of charge and unpaired electron, are well separated in energy, and show a very clear preference for the formation of GeH_3^- and the CH_2CHCH_2 radical fragments. The opposite dissociation mode, which produces an allyl anion fragment and a germyl radical, is 29.3 kcal mol^{-1} higher in energy at the CCSD(T) level of calculation (and 24.7 kcal mol^{-1} at CASPT2). These results can be compared with the energy difference obtained from the experimental electron affinities of the allyl and germyl radicals, 29 kcal mol^{-1} [87][4]. It is possible that some cancellation of errors contributes to the rather close agreement between the two values[5].

The maximum along the CCSD(T) energy profile corresponds to a barrier of ca. 4 kcal mol^{-1} (somewhat higher than 5 with the more extended basis set) with respect to the more stable tbp eq minimum (Fig. 4). This energy maximum precedes geometrically the dissociation limit, and is very close to the dissociation limit, which lies at ca. 4 kcal mol^{-1} (almost 6 with the more extended basis set) above the minimum. The dissociation limit is at 8.7 kcal mol^{-1} above the reactant at the CAS(5,4)-PT2/6-311+G(2d,p) level of theory.

The minimum on the energy profile between the transition structure and the dissociation limit corresponds to a ion-dipole electrostatic complex (the Ge distance from the closest carbon is ca. 4 Å), the association of the allyl radical with the germyl anion (as results from the charges and spin densities: $Q(GeH_3) = -1.0019$ and $\Delta P(GeH_3) = 0.0001$). This minimum is located less than 1 kcal mol^{-1} above the initial radical anion at the CCSD(T)/6-311+G(d) level of calculation. The qualitative features of the dissociation energy profile are similar to those of the analogous C or Si systems [47].

[4] Compare also the IE and EA data available on the NIST site (http://webbook.nist.gov/). Allyl. EA=0.481 eV, from [88]. Pentadienyl. EA=0.91 eV, from [89]. Germyl. EA = 1.739 eV see [80].

[5] The discrepancy is largely due to basis set deficiencies. In fact, we carried out some tests on these molecules at the CCSD(T) level with basis sets of increasing size, up to 6-311++G(3df,2p), and found significant improvements in approaching the experimental data. Unfortunately, at the CCSD(T) level, the 6-311+G(2d,p) is the largest affordable basis set for the heaviest systems dealt with in this paper. On the other hand, when estimating either the energy differences between different dissociation limits or the activation effects, some cancellations produce a better agreement with the same values assessed by using the experimental data.

Table 1 Allylgermane radical anion: energy differences for the dissociation process

	CAS(9,8)-MCSCF		CCSD(T)		CAS(5,4)-PT2
	6-31G(d)	6-311G(d)	6-311+G(d)	6-311+G(2d,p)	6-311+G(2d,p)
Tbp eq	0.0	0.0	0.0	0.0	0.0
Tbp ax	2.6	–	4.6	–	8.3
Dissociation TS from tbp eq[a]	0.1	3.2	4.3	5.3	0.3
Allyl radical + germide	−10.1	1.4	4.1	5.9	8.7
Allyl anion + germyl	40.7	–	33.4	–	33.4

Values are kcal mol^{-1}; CASSCF optimizations, coupled cluster and CASPT2 single point energy evaluations on the CASSCF geometries (see text)
[a] For the coupled cluster and CASPT2 calculations, this value refers to the energy maximum along the dissociation energy profile, not to the geometry of the CASSCF TS

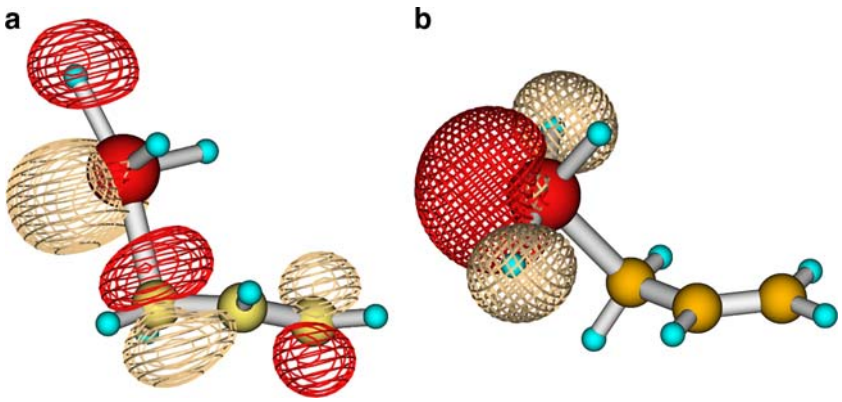

Fig. 3 SOMOs of the tbp eq **a** and tbp ax **b** allylgermane radical anions. In the latter, a C–Ge antibonding trait cannot be observed (see also the different C–Ge bond lengths in Fig. 2)

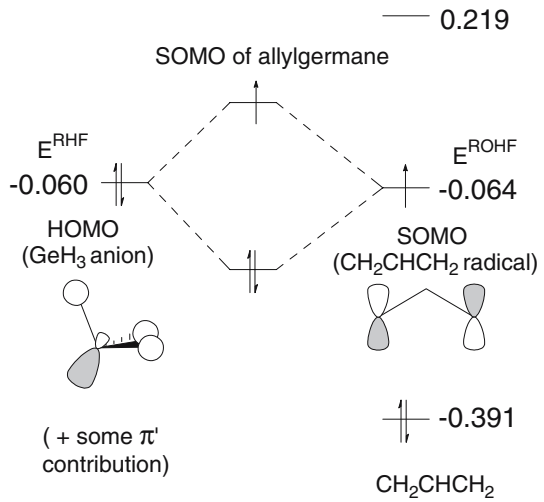

Chart 3 Out-of-phase interaction of the germide HOMO with the allyl radical SOMO to give the allylgermane SOMO

3.2.1 Activation toward dissociation

The coupled cluster data for the radical ions and their fragmentation products show that the reaction is remarkably easier than the homolytic process in the parent neutral system. In fact, homolysis of allylgermane requires a very large energy: 62 kcal mol^{-1} (Scheme 2, left). The homolytic dissociation profile is entirely determined by the reaction energy in that it does not show a barrier for the reverse process (no kinetic "overhead"). In contrast, the fragmentation of the corresponding radical anion has been seen to require an energy of ca. 4 kcal mol^{-1}. The radical anion is higher in energy than the neutral by 30 kcal mol^{-1}, at the same computational level. The two dissociation limits are separated by 28 kcal mol^{-1}.

These energy differences result in an *activation* effect toward dissociation, which we label in the following ΔE_A, with respect to homolysis in the neutral. It can be assessed as 58 kcal mol^{-1}. The origin of this cleavage activation is due in part to reactant destabilization, in part to the positioning of the dissociation limit (in passing from germyl to germide). Actually, the computed energy difference between germide and germyl seems underestimated when compared to the experimental EA of the germyl radical, 40.1 kcal mol^{-1} [87]. A similar underestimation could be also present in the allyl germane radical anion calculation, but no experimental datum is available. This discrepancy had also been observed in the study of the analogous carbon and silicon radical anions (see the comments in Ref. [47], note 43). In spite of this systematic [47] apparent underestimation, we can comment on the trends in ΔE_A estimated for the carbon, silicon and germanium systems. There is evident increase of this effect along the series. In the allyl-XH_3 radicals anions, the energy required to dissociate drops to 36% (X=C), 19% (X=Si) and just 6% (X=Ge) of the energy required for C−X bond homolysis

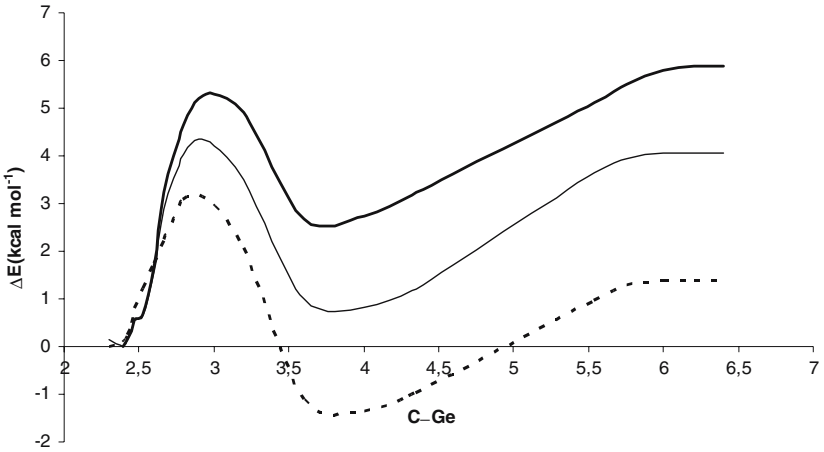

Fig. 4 Coupled cluster energy profiles for the dissociation of allylgermane radical anion (tbp eq). C–Ge distances in Ångströms. *Dashed line* CCSD(T)/6-311G(d) values. *Thin continuous line* CCSD(T)/6-311+G(d) values. *Thick continuous line* CCSD(T)/6-311+G(2d,p) values. The reactant energies have been set to coincide

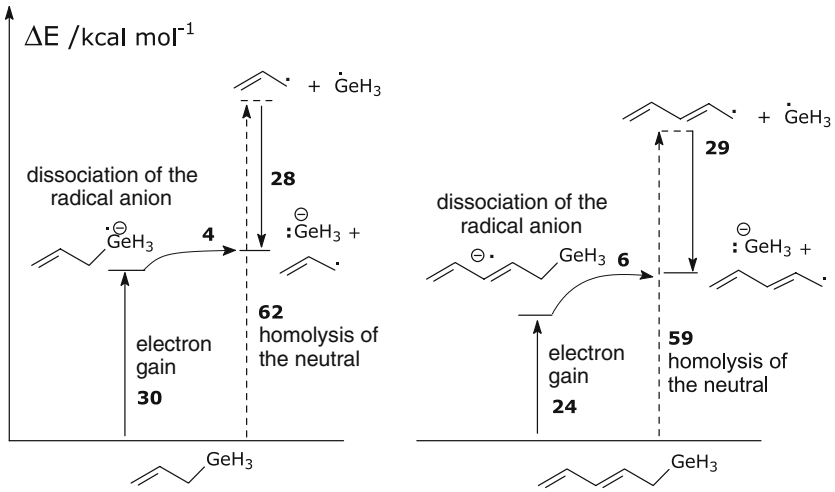

Scheme 2 *Activation* of the radical anions toward dissociation: in allylgermane $\Delta E^{\ddagger}$ plummets from 62 to 4 kcal mol^{-1}, in pentadienylgermane from 59 to 6 kcal mol^{-1})

of the parent neutral systems. The qualitative trend is clear, and the effect in the germanium system is quite dramatic.

3.2.2 Nature of the dissociation

It can be seen in Fig. 2 that the negative charge in the reactant is in part associated to the allyl component of the radical ion, in part to the germyl component (charge distribution computed as NAO group charges) [27–35]. This suggests that two limit forms might be written down for the reagent, one having the charge localized on the germyl group, the other on the double CC bond (Scheme 3).

If the dissociation mode of the allylgermane radical anion into allyl radical and germyl anion is taken into account, the upper resonance structure indicates homolytic cleavage (but along with a spin recoupling), while the bottom structure suggests heterolytic cleavage.

The analysis of the CI wave function Ψ is helpful for a better understanding of the nature of the dissociation process. It can be carried out in terms of coefficients of the lowest eigenvector and population of the active orbitals $(\gamma)_i$. A single configuration dominates Ψ all along the reaction pathway

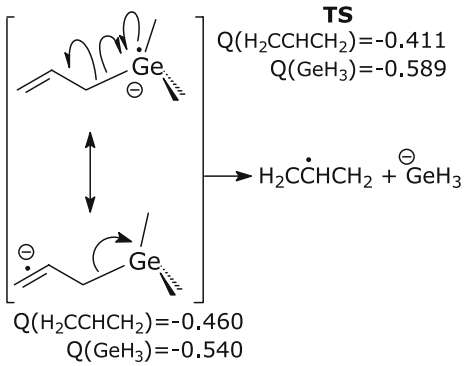

Scheme 3 Resonance structures for the allylgermane radical anion. *Arrows* in the first one would suggest homolytic cleavage with spin recoupling, in the second one, heterolytic cleavage

(for instance the highest coefficient is larger than 0.95 in the transition structure) and the fractional populations of the eight active orbitals γ_i are rather close to 0, 1 and 2. For instance, in the transition structure, the populations of the active orbitals are $\gamma_1 = 1.969, \gamma_2 = 1.919, \gamma_3 = 1.973, \gamma_4 = 1.989, \gamma_5 = 1.007, \gamma_6 = 0.034, \gamma_7 = 0.027$ and $\gamma_8 = 0.083$. This picture is clearly different from what is charac-

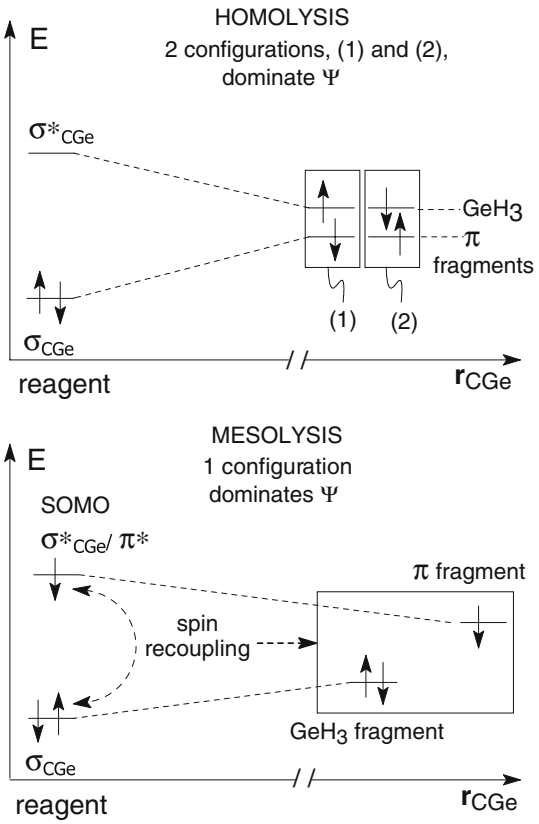

Scheme 4 Allylgermane radical anion: spin coupling patterns featured by the homolytic and mesolytic dissociations (tetrahedral or trigonal bipyramidal arrangement around Ge)

teristic of homolysis (two electron configurations acquiring comparable weight as the bond is stretched). The dissociation mode of the allylgermane radical anion could seem closer to heterolysis, in which one configuration dominates at all distances and no electron pair is disrupted. However, the monoconfigurational nature of Ψ can be attributed to the spin pairing of the originally unpaired electron with one of the electrons of the cleaving bond, which is a distinctive feature of bond cleavage in a radical anion (Scheme 4). The overall description seems to further justify the use of the word *mesolysis* for this kind of process.

In the dissociation TS, the unpaired electron occupies an orbitals which is a combination of σ^* and π^* orbitals, characterized by the contribution of the $\sigma^*_{\mathrm{Ge-C}}$ component (compare Fig. 3). Then, as the C–Ge bond undergoes a further stretching, the single electron goes to occupy an orbital largely characterized by the contribution of the π^* component.

3.3 Pentadienylgermane radical anion

At the CAS-MCSCF(7,6) level of theory, two energy minima are found on the energy surface. When the radical anion shows a trigonal bipyramidal arrangement around Ge, the extra electron is significantly located on the germyl group associated, however, to a molecular orbital with a rather large lobe on Ge and antibonding character between germanium and the carbon bound to it, as in the smaller systems (Sects. 3.1 and 3.2). This lobe is in an axial position (tbp ax, Fig. 5). A tbp eq minimum could not be found, at variance with the preceding case and with the methylgermane system (Sect. 3.1). The second (and more stable, Table 2) structure has a tetrahedral disposition of the atoms bound to Ge (Fig. 6).

This minimum is lower in energy than tbp ax by 6.8 kcal mol^{-1} (CCSD(T) values). The extra electron is more associated to the unsatured part of the radical anion (Fig. 7), which is a better acceptor than in the preceding case (the more extended a conjugated system is, the lower in energy its lowest unoccupied π^*_{CC} orbitals). Note the bond lengths of the double CC bonds in Figs. 5 and 6. We can observe that, though the SOMO of this tetrahedral-Ge structure has some antibonding character with regard to the Ge−C bond, as seen in the bpt eq allylgermane radical anion, its π component has the same phases as the LUMO of a diene, at variance with the characteristics exhibited by the smaller bipyramidal system.

The two dissociation limits (pentadienyl + germide and pentadienide + germyl) are again separated in energy by

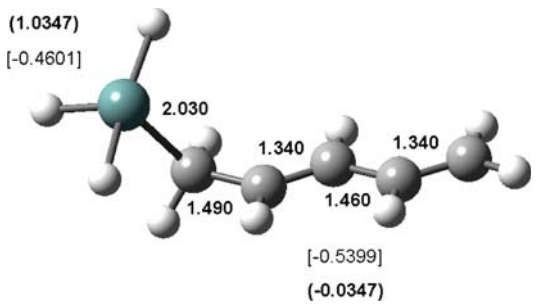

Fig. 5 The pentadienyl germane radical anion stable structure with a trigonal bipyramidal arrangement around Ge. Some selected bond lengths, and NAO group charges (between brackets) for the germyl and allyl parts of the system. UHF group spin densities in parentheses

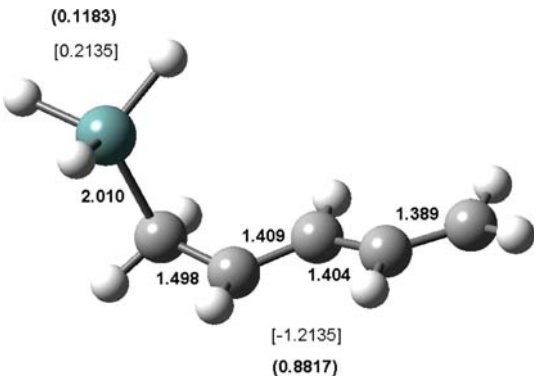

Fig. 6 The pentadienyl germane radical anion stable structure with a tetrahedral arrangement around Ge, and the extra electron on the unsaturated region. Some selected bond lengths and the NAO group charges, between brackets, for the germyl and pentadienyl parts of the system. UHF group spin densities in parentheses

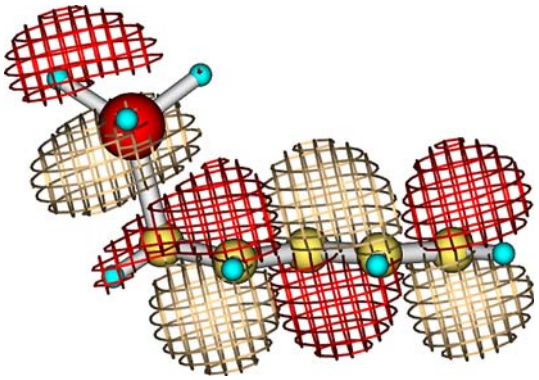

Fig. 7 SOMO of the pentadienylgermane radical anion with tetrahedral $H_3Ge(C)$ arrangement

Table 2 Pentadienylgermane radical anion: energy differences for the dissociation process

	CAS(7,6)-MCSCF 6-31G(d)	CCSD(T) 6-311+G(d)
Tetrahedral	3.9	0.0
Tetrah. to ax TS[a]	–	1.2
Tbp ax	0.0	−0.1
Dissociation TS[a]	5.0	–
Pentadienyl radical + germide	−17.3	5.8
Pentadienide + germyl	20.7	24.5

Values are kcal mol^{-1}; CASSCF optimizations, coupled cluster and CASPT2 single point energy evaluations on the CASSCF geometries (see text)

[a] For the coupled cluster calculations, this value refers to the energy maximum along the dissociation energy profile, not to the geometry of the CASSCF TS

a significant amount, 18.7 kcal mol^{-1} (in the allyl case by 29.3 kcal mol^{-1}). This result can be compared with the energy difference of 19.1 kcal mol^{-1}, obtained from the experimental EAs of the germyl and pentadienyl radicals [88,89]. Also in this case the computational and experimental results appear to be in good agreement.

The fragmentation, starting from of the tetrahedral minimum, proceeds by stretching the C−Ge bond, through a rather low energy barrier of 1.2 kcal mol^{-1} (Fig. 8). This leads to the other stable structure, with a trigonal bipyramidal arrangement. In the transition structure, when the C−Ge bond distance is still 2.13–2.16 Å, the unpaired electron still occupies an orbital characterized by the contribution of the lowest π^* component of the pentadienyl fragment. However, upon further elongation of the C−Ge bond distance (around $r_{C-Ge} = 2.30$ Å) the electron occupies an orbital characterized by the contribution of the σ^*_{C-Ge} component. On the CCSD(T) energy profile, no trace of a ion-dipole complex minimum is kept. The reaction energy at the CCSD(T)/6-311+G(d) is 5.8 kcal mol^{-1} (Fig. 8).

3.3.1 Activation toward dissociation

Also the pentadienylgermane radical anion dissociation is activated with respect to the homolytic process in the parent neutral system (Scheme 2, right). Homolysis of the C−Ge bond in pentadienilgermane requires 59 kcal mol^{-1}. The same cleavage in its radical anion is estimated to require only 6 kcal mol^{-1}. The dissociation limit corresponding to pentadienyl radical plus germide is lower than the homolytic dissociation limit by 29 kcal mol^{-1}. These data bring about an activation effect, with respect to homolysis in neutral, of 53 kcal mol^{-1}. Again, the computed energy difference is smaller than the experimental germyl EA value, 40 kcal mol^{-1} [88,89]. However, we can consider the qualitative trends for ΔE_A in the pentadienyl-XH_3 series (the hexa-1,3-dienyl radical anion, X=C, the penta-2,4-dienylsilyl radical anion, X=Si, and the penta-2,4-dienylgermyl radical anion, X=Ge). We can note a clear increase for ΔE_A, and the energy required to dissociate decreases consistently to

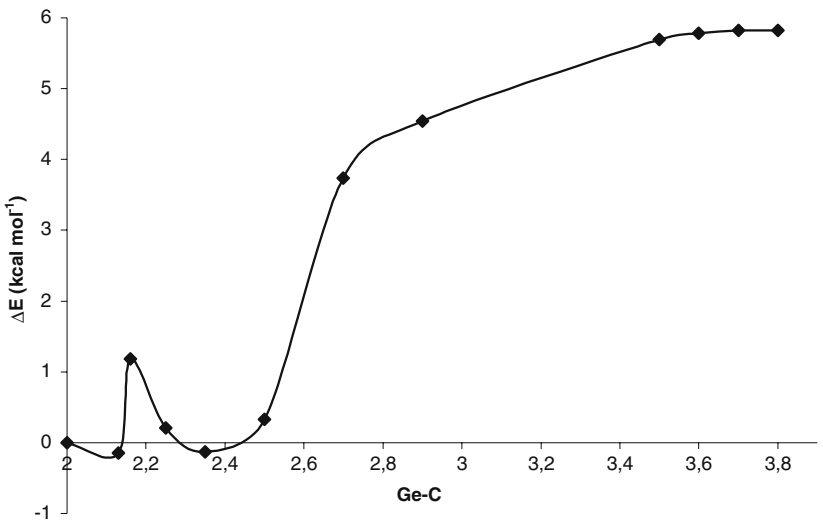

Fig. 8 Coupled cluster energy profiles for the dissociation of pentadienylgermane radical anion. CCSD(T)/6-311+G(d) energy values. C–Ge distances in Ångströms

44% (X=C), 19% (X=Si) and 10% (X=Ge). The effect in the germanium system is again sizeable.

3.3.2 Nature of dissociation

The CAS-MCSCF charge distribution, which in the smaller radical ion can be reflected by two resonance structures, corresponds here to distinct stable structures with different geometries. It can be seen in Fig. 5 that in the tetrahedral-Ge reactant the negative charge is fully associated with the unsaturated component of the radical ion ($Q_{NAO} = -1.213$). In the relevant transition structure the negative charge is partially transferred from the π-system ($Q_{NAO} = -0.997$) to the tetrahedral germyl group. By contrast, in the tbp ax structure of the reactant the charge is more heavily associated to the germyl group. From the analysis of the CI wave function (Ψ), a single configuration stands out at all interfragment distances. In the transition structure the highest coefficient is larger than 0.96, and the fractional population of the active orbitals (γ_i) are rather close to 0, 1 or 2 ($\gamma_1 = 1.982$, $\gamma_2 = 1.966$, $\gamma_3 = 1.938$, $\gamma_4 = 1.010$, $\gamma_5 = 0.065$, $\gamma_6 = 0.038$). The spin recoupling of one of the two C–Ge bond electrons with the unpaired electron points out that the dissociation process is basically different from homolytic or heterolytic cleavage.

4 Conclusions

In this study two radical anions of germyl-substituted alkenes have been examined.

(1) It has been found that the extension of the π system is crucial in determining the possibility of accepting the extra electron either on the germyl part only of the molecule, or mainly on the unsaturated carbon skeleton. In fact, the allylgermane radical anion is unable to accept the extra electron in its lowest unoccupied π^*_{CC} orbital; In contrast the pentadienyl-germane radical anion does it, and the germyl group stays tetrahedral as in the neutral parent molecule. On the other hand, when Ge assumes a trigonal bipyramidal arrangement, both can locate this electron in an orbital with σ^*_{CGe} character, having also a significant contribution by a Ge lobe.

(2) The origin of the cleavage activation observed in the hypernomers with respect to their neutral precursors is due in part to reactant destabilization, in part to the energetic positioning of the dissociation limit (in passing from germyl to germide, which is lower in energy).

(3) The nature of the fragmentation process. One configuration dominates at all distances. This trait would set this bond cleavage close to heterolysis, in which no electron pair is disrupted. However, the spin pairing of the originally unpaired electron with one of the electrons of the cleaving bond is an extra feature which can be held accountable for the monoconfigurational nature of Ψ. On the other hand, this bond cleavage is evidently at variance with homolysis, in which two electron configurations acquire comparable weight as the bond is stretched.

(4) Comparison with the silicon (or carbon) counterparts of the two germanium radical anions. Of course, only silicon was capable of assuming a trigonal bipyramidal arrangement. We note an increase of the activation effect along the series C, Si, Ge. For instance, in the allyl-XH_3 radicals anions, the energy required to dissociate drops to 36% (X=C), 19% (X=Si) and just 6% (X=Ge) of the energy required for C−X bond homolysis of the parent neutral systems. The effect in the allyl-GeH_3 system is quite dramatic. The reactions are also less endoergic in the same order. The Si and Ge systems prefer to dissociate giving silide and germide, respectively, while the analogous carbon system gives preferentially a methyl radical.

Acknowledgements Financial support was provided by the Italian MIUR through the "Cofinanziamento di Programmi di Ricerca di Rilevante Interesse Nazionale 2005", within the project "Experimental and Theoretical Study of Gaseous Systems: Reactivity, Comparison with the Condensed Phase and Formation of Amorphous Solids".

References

1. Albini A, Mella M, Freccero M (1994) Tetrahedron 50:575–607 (Tetrahedron Report N. 348), and reference therein
2. Lew CSQ, Brisson JR, Johnston LJ (1997) J Org Chem 62:4047–4056
3. Pandey G, Gadre SR (2004) Acc Chem Res 37:201–210
4. Zheng Z-R, Evans DH, Chan-Shing ES, Lessard J (1999) J Am Chem Soc 121:9429–9434
5. Andersen ML, Mathivanan N, Wayner DDM (1996) J Am Chem Soc 118:4871–4879
6. Andrieux CP, Savéant J-M, Tallec A, Tardivel R, Tardy C (1997) J Am Chem Soc 119:2420–2429
7. Constentin C, Hapiot P, Médebielle M, Savéant J-M (1999) J Am Chem Soc 121:4451–4460
8. Closs GL, Calcaterra LT, Green NJ, Penfield KW, Miller JR (1986) J Phys Chem 90:3673–3683
9. Meot-Ner N, Neta P, Norris RK, Wilson K (1986) J Phys Chem 90:168–173
10. Chiavarino B, Crestoni ME, Fornarini S (2000) Organometallics 19:844–848
11. Born M, Ingemann S, Nibbering NMM (1997) Mass Spectr Rev 16:181–200
12. Pisano L, Farriol M, Asensio X, Gallardo I, Gonzáles-Lafont A, Lluch JM, Marquet J (2002) J Am Chem Soc 124:4708–4715
13. Asensio X, Gallardo I, Gonzáles-Lafont A, Lluch JM, Marquet J (2005) J Org Chem 70:540–548
14. Costentin C, Robert M, Savéant J-M (2004) J Am Chem Soc 126:16834–16840
15. Pandey G, SeshaPoleswara Rao KS, Palit DK, Mittal JP (1998) J Org Chem 63:3968–3978
16. Rossi RA, Pierini AB, Santiago AN in Organic reactions, Paquette L A, Bittman R (eds) Wiley, New York (1999) 1
17. Rossi RA, Peñéñory AB, Pierini AB (2003) Chem Rev 103:71–167
18. Yammal CC, Podestá JC, Rossi RA (1992) J Org Chem 57:5720–5725

19. Tanner DD, Chen JJ, Chen L, Luelo C (1991) J Am Chem Soc 113: 8074–8081
20. Tanner DD, Stein AR (1988) J Org Chem 53:1642–1646
21. Tanko JM, Brammer LE, Hervas M, Campos K (1994) J Chem Soc Perkin Trans 2:1407–1409
22. Chanon M, Rajzmann M, Chanon F (1990) Tetrahedron 46:6193–6299 (Tetrahedron Report#280), and references therein
23. Maslak P, Narvaez JN (1990) Angew Chem Int Ed Engl 29:283–285
24. Maslak P, Vallombroso TM, Chapman WH Jr, Narvaez JN (1994) Angew Chem Int Ed Engl 33:73–75, and references therein
25. Maslak P, Theroff J (1996) J Am Chem Soc 118:7235–7236
26. Arnett EM, Venimadhavan S (1991) J Am Chem Soc 113:6967–6975
27. Zhang X-M, Bordwell FG, Bares JE, Cheng J-P, Petrie BC (1993) J Org Chem 58:3051–3059
28. Bunnet JF, Creary X (1975) J Org Chem 40:3740–3743
29. Adcock W, Clark CI, Houmam A, Krstic AR, Pinson J, Savéant J-M, Taylor DK, Taylor JF (1994) J Am Chem Soc 116:4653–4659
30. Popielarz R, Arnold DR, Du XJ (1990) Am Chem Soc 112:3068–3082
31. Zhang X-M, Bordwell FG (1994) J Am Chem Soc 116:904–908
32. Ichinose N, Mizuno K, Otsuji Y, Tachikawa H (1994) Tetrahedron Lett 35:587–590
33. Zhang X-M (1993) J Chem Soc Perkin 2:2275–2279
34. Zhang X-M, Bordwell FG (1992) J Am Chem Soc 114: 9787–9792
35. Savéant J-M (2000) Adv Phys Org Chem, Tidwell TT (ed) Academic, New York p 35, and references therein
36. Villar H, Castro EA, Rossi RA (1982) Can J Chem 60:2525–2527
37. Takahashi O, Kikuchi O (1991) Tetrahedron Lett 32:4933–4936
38. Takahashi O, Morihashi K, Kikuchi O (1990) Tetrahedron Lett 31:5175–5178
39. Du X, Arnold DR, Boyd RJ, Shi Z (1991) Can J Chem 69:1365–1375
40. Arnold DR, Du X (1989) J Am Chem Soc 111:7666–7667
41. Camaioni DM (1990) J Am Chem Soc 112:9475–9483
42. Pierini AB, Vera DMA (2003) J Org Chem 68:9191–9199
43. Anusiewicz I, Sobczyk M, Berdys-Kochanska J, Skurski P, Simons J (2005) J Phys Chem A 109:484–492
44. Antonello S, Benassi R, Gavioli G, Taddei F, Maran F (2002) J Am Chem Soc 124:7529–7538
45. Konovalov VV, Laev SS, Beregovaya IV, Shchegoleva LN, Shteingarts VD, Tsvetkov YD, Bilkis I (2000). J Phys Chem A 104:352–361
46. Carra C, Fiussello F, Tonachini G (1999) J Org Chem 64:3867–3877
47. Carra C, Ghigo G, Tonachini G (2003) J Org Chem 68:6083–6095
48. Csizsmadia IG, Daudel R (eds) Computational theoretical organic chemistry, Reidel 1981, p 129–159
49. Schlegel HB (1982) J Chem Phys 77:3676–3681
50. Schlegel HB, Binkley JS, Pople JA (1984) J Chem Phys 80:1976–1981
51. Schlegel HB (1982) J Comput Chem 3:214–218
52. Roos B (1987) The complete active space self-consistent field method and its applic-ations in electronic structure calculations. In: Lawley KP (ed) Ab initio methods in quantum chemistry-II, Wiley, New York
53. Hegarty D, Robb MA (1979) Mol Phys 38:1795–1812
54. Robb MA, Eade RHA (1981) NATO Adv Study Inst Ser C 67:21–54
55. Hehre WJ, Ditchfield R, Pople JA (1972) J Chem Phys 56:2257–2261
56. Hariharan PC, Pople JA (1973) Theor Chim Acta 28:213–222
57. Clark T, Chandrasekhar J, Spitznagel GW, Schleyer PvR (1983) J Comput Chem 4:294–301
58. Krishnan R, Binkley JS, Seeger R, Pople JA (1980) J Chem Phys 72:4256–4266
59. Frisch MJ, Pople JA, Binkley JS (1984) J Chem Phys 80:3265–3269
60. Carpenter J E, Weinhold F (1988) J Mol Struct (Theochem) 169:41
61. Carpenter JE PhD thesis, University of Wisconsin, Madison, 1987
62. Foster JP, Weinhold F (1980) J Am Chem Soc 102:7211
63. Reed AE, Weinhold F (1983) J Chem Phys 78:4066
64. Reed AE, Weinstock RB, Weinhold F (1985) J Chem Phys 83:735
65. Reed AE, Curtiss LA, Weinhold F (1988) Chem Rev 88:899
66. Roos BO, Andersson K, Fülscher MP, Malmqvist P-Å, Serrano-Andres L, Pierloot K, Mercham M (1996) Adv Chem Phys 93:219–331
67. Andersson K, Malmqvist P-Å, Roos BO (1992) J Chem Phys 96:1218–1226
68. Coester F, Kümmel H (1960) Nucl Phys 17:477
69. Cízek J (1966) J Chem Phys 45:650–654
70. Paldus J, Cízek J, Shavitt I (1972) Phys Rev A 5:50–67
71. Pople JA, Krishnan R, Schlegel HB, Binkley JS (1978) Int J Quantum Chem 14:545–560
72. Bartlett RJ, Purvis GD (1978) Int J Quantum Chem 14:561–581
73. Cízek J, Paldus J (1980) Phys Scripta 21:251–254
74. Bartlett RJ (1981) Ann Rev Phys Chem 32:359–401
75. Purvis GD, Bartlett RJ (1982) J Chem Phys 76:1910–1918
76. Scuseria GE, Janssen CL, Schaefer HFIII (1988) J Chem Phys 89:7382–7387
77. Scuseria GE, Schaefer HFIII (1989) J Chem Phys 90:3700–3703
78. Frisch MJ, Trucks GW, Schlegel HB, Scuseria GE, Robb MA, Cheeseman JR, Montgomery JA Jr, Vreven T, Kudin KN, Burant JC, Millam JM, Iyengar SS, Tomasi J, Barone V, Mennucci B, Cossi M, Scalmani G, Rega N, Petersson GA, Nakatsuji H, Hada M, Ehara M, Toyota K, Fukuda R, Hasegawa J, Ishida M, Nakajima T, Honda Y, Kitao O, Nakai H, Klene M, Li X, Knox JE, Hratchian HP, Cross JB, Adamo C, Jaramillo J, Gomperts R, Stratmann RE, Yazyev O, Austin AJ, Cammi R, Pomelli C, Ochterski JW, Ayala PY, Morokuma K, Voth GA, Salvador P, Dannenberg JJ, Zakrzewski VG, Dapprich S, Daniels AD, Strain MC, Farkas O, Malick DK, Rabuck AD, Raghavachari K, Foresman JB, Ortiz JV, Cui Q, Baboul AG, Clifford S, Cioslowski J, Stefanov BB, Liu G, Liashenko A, Piskorz P, Komaromi I, Martin R L, Fox DJ, Keith T, Al-Laham MA, Peng CY, Nanayakkara A, Challacombe M, Gill PMW, Johnson B, Chen W, Wong MW, Gonzalez C, Pople JA, (2003) Gaussian 03, Revision B.02, Gaussian, Pittsburgh
79. MOLCAS 4: Andersson K, Blomberg MRA, Fülscher MP, Karlström K, Lindh R, Malmqvist P-Å, Neogrády P, Olsen J, Roos BO, Sadlej AJ, Schütz M, Seijo L, Serrano-Andrés L, Siegbahn PEM, Windmark P-O (1997) MOLCAS Version 4, University of Lund, Sweden
80. Vera DMA, Pierini AB (2004) Phys Chem Chem Phys 6:2899–2903
81. Dézarnaud-Dandine C, Sevin A (1996) J Am Chem Soc 118:4427–4433
82. Dézarnaud-Dandine C, Bournel F, Tronc M, Jones D, Modelli A (1998) J Phys B Mol Opt Phys 31:L497–L502, and references therein
83. Falcetta MF, Jordan KD (1990) J Phys Chem 94:5666–5669
84. Guerra M (1999) J Phys Chem 103:5983–5988
85. Alberti A, Barberis C, Campredon M, Gronchi G, Guerra M (1995) J Phys Chem 99:15779–15784
86. Guerra M (1992) Chem Phys Lett 197:205–212
87. Lias SG, Bartmess JE, Liebman JF, Holmes JL, Levin RD, Mallard WG (1988) J Phys Chem Ref Data Suppl 17
88. Wenthold PG, Polak ML, Lineberger WC (1996) J Phys Chem 100:6920
89. Zimmerman AH, Gygax R, Brauman JI (1978) J Am Chem Soc 100:5595